Description of Nonlinear Optical Response Using Phase Space Wave Packets

Yoshitaka Tanimura and Shaul Mukamel*

Department of Chemistry, University of Rochester, Rochester, New York 14627

Received: June 21, 1993®

Closed-form expressions are derived for the nonlinear response function of a polyatomic molecule with two electronic states and linearly displaced harmonic potentials to arbitrary order in the radiation field. The underlying dynamics can be best visualized using wave packets in phase space. Using exact expressions for these wave packets, we discuss the possible factorization of the process into two parts representing a forward and a backward propagating wave packet. This factorization facilitates the description of sequential measurements, such as pump–probe spectroscopy, in terms of a doorway wave packet prepared by the pump and a window prepared by the probe. We show that once a reduced description is adopted, where we trace over bath degrees of freedom, this factorization is possible only in certain limiting cases.

I. Introduction

The density matrix offers a natural and convenient means for calculating and interpreting ultrafast optical measurements.[1-4] This is well recognized for studies in the condensed phase, since it allows performing thermal averaging and developing a reduced description in which bath coordinates have been eliminated and replaced by dephasing processes. However, even for isolated molecules in the gas phase, the density matrix formulation has a lot to offer compared with wave function based calculations.[5]

The density matrix follows naturally the time ordering of the various interactions with the fields. In the Wigner representation, it can be used to construct a phase–space wave packet representation of the nonlinear response which provides a powerful framework for developing classical and semiclassical approximations.[2] The possibility of visualizing time domain spectroscopy in terms of wave packets in phase space is particularly valuable for sequential experiments such as pump–probe, transient grating, and impulsive Raman scattering conducted using well-separated laser pulses[6-11] Sequential experiments can be described in terms of overlap of two wave packets in phase space (the doorway window picture).[2,3] A full quantum treatment of these wave packets in the complete phase space (when all degrees of freedom are included) has been developed.[5] This level of description is restricted to small systems (e.g., pump–probe spectroscopy of ICN in the gas phase).[3] For larger systems and for spectroscopy in the condensed phase, we need to develop a reduced description in which only part of the phase space is treated explicitly and the remaining degrees of freedom are eliminated. Using a Langevin equation, Yan and Mukamel have calculated the wave packets for a multimode Brownian oscillator model.[2] These calculations are limited by the Langevin equation which provides a semiclassical high-temperature approximation. We recently developed a theory for the nonlinear optical response of a multimode Brownian oscillator model which extends that theory in the following respects: First, by adopting a harmonic model for the bath degrees of freedom, we derived exact quantum expressions for the phase space wave packets which are valid at all temperatures and for the entire range of parameters. The solution was obtained using path integral techniques. Second, we calculated the response function to arbitrary order in the field so that we can describe processes higher than four-wave mixing. Third, we incorporated an arbitrary dependence of the transition dipole on nuclear coordinates (non-Condon effects).

In this article, we use the exact solution of the multimode Brownian oscillator model to explore the applicability of the doorway–window picture for sequential measurements. We show that once a reduced description is adopted, where we trace over bath degrees of freedom, this representation is possible only in certain limiting cases.

II. Nuclear Response Function of a Multimode Harmonic System

We consider a polyatomic molecule with two electronic states denoted g (the ground state) and e (the excited state) and with frequency ω_{eg}^0. We assume that both ground- and excited-state potential surfaces are harmonic, with a displaced equilibrium position between the two states. We denote a nuclear mass, coordinate, harmonic frequency, and a dimensionless displacement of the potential for the sth optically active vibration by m_s, q_s, ω_s, and D_s, respectively. The Hamiltonian is then given by (see Figure 1)

$$H \equiv |g\rangle H_g(\mathbf{p},\mathbf{q})\langle g| + |e\rangle H_e(\mathbf{p},\mathbf{q})\langle e| - VE(t) \tag{1}$$

where

$$\begin{cases} H_g(\mathbf{p},\mathbf{q}) = \sum_s \left[\dfrac{p_s^2}{2m_s} + \dfrac{1}{2} m_s \omega_s^2 q_s^2 \right] \\ H_e(\mathbf{p},\mathbf{q}) = \hbar\omega_{eg}^0 + \sum_s \left[\dfrac{p_s^2}{2m_s} + \dfrac{1}{2} m_s \omega_s^2 (q_s - D_s)^2 \right] \end{cases} \tag{2}$$

The transition dipole operator V is written as

$$V \equiv \sum_s \mu_s (|g\rangle\langle e| + |e\rangle\langle g|) \equiv \mu(|g\rangle\langle e| + |e\rangle\langle g|) \tag{3}$$

Here, we set $\mu \equiv \sum_s \mu_s$, where μ_s is the dipole matrix element for the sth mode. We assume that μ_s does not depend on nuclear coordinate (the Condon approximation). However, our discussion can be extended to the non-Condon case, which plays an important role for off-resonance laser excitation.[4,8,9] The system is initially at equilibrium in the ground electronic state:

$$\rho_g = |g\rangle\langle g| \exp[-\beta H_g]/\mathrm{Tr}\{\exp[-\beta H_g]\} \tag{4}$$

where $\beta \equiv 1/k_B T$ is the inverse temperature.

The optical response can be expressed in terms of the optical polarization

$$P(t) \equiv \mathrm{tr}\{V\rho(t)\} \tag{5}$$

where $\rho(t)$ is the density matrix which depends on the interaction between the driving field and the system. For sufficiently weak fields, the polarization may be expanded in powers of the electric field $E(t)$. All even orders of the polarization vanish for the

• Abstract published in *Advance ACS Abstracts*, November 1, 1993.

0022-3654/93/2097-12596$04.00/0 © 1993 American Chemical Society

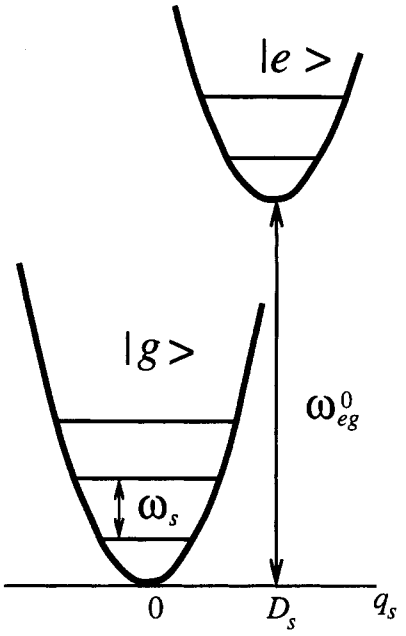

Figure 1. Potential surfaces of the linearly displaced harmonic oscillator system. The lower state is denoted |g⟩, and the upper is |e⟩. The equilibrium coordinate displacement and the energy difference between two potentials are expressed by D_s and $\hbar\omega_{eg}^0$, respectively.

present model. The odd order components are given by[4]

$$P^{(2N-1)}(t) = \left(\frac{-i}{\hbar}\right)^{2N-1} \int_0^\infty dt_{2N-1} \int_0^\infty dt_{2N-2} \cdots \int_0^\infty dt_1 \times \mu^{2N} E(t-t_{2N-1})\, E(t-t_{2N-1}-t_{2N-2}) \cdots E(t-t_{2N-1}- \cdots -t_1) \times \sum_\alpha R_\alpha^{(2N-1)}(\mathbf{t}) \quad (6)$$

where $\mathbf{t} = \{t_{2N-1}, t_{2N-2}, \ldots, t_1\}$ and

$$R_\alpha^{(2N-1)}(\mathbf{t}) \equiv \exp\left[\sum_s Q_\alpha^s(\mathbf{t})\right] \quad (7)$$

is the nonlinear response function with $Q_\alpha^s(\mathbf{t})$ given in Appendix A. The response function contains 2^{2N-1} terms $R_\alpha^{(2N-1)}(\mathbf{t})$ denoted *Liouville space paths*. They come from taking $2N-1$ commutators with the dipole operator in the evaluation of the density matrix. In each path, the system undergoes $2N-1$ evolution periods denoted chronologically by $t_1, t_2, \ldots, t_{2N-1}$. The paths differ by which electronic density matrix element exists in each of these periods. Mathematically, we can represent the path by $2N-1$ indices ϵ_j (*i.e.*, $\alpha \equiv \{\epsilon_j\}$), which are chosen as follows: When the density matrix during the jth period t_j is in the state ρ_{gg}, ρ_{ee}, ρ_{eg}, and ρ_{ge}, we chose $\epsilon_j = -1, +1, +1$, and -1, respectively. The summation in the above equation, $\sum_\alpha$, represents the sum for possible sign $\epsilon_1, \epsilon_2, \ldots, \epsilon_{2N-1} = \pm$, which yields the necessary 2^{2N-1} Liouville space paths. In practice, we need only half of the terms by choosing, say, with $\epsilon_{2N-1} = +1$. The others are simply their complex conjugates. As an example, let us consider the third-order polarization $P^{(3)}(t)$ ($N = 2$). In this case, we need to consider four Liouville space paths. The double-sided Feynman diagrams representing these paths are displayed in Figure 2. They are listed in Table I together with the corresponding indices of ϵ_1, ϵ_2, and ϵ_3. For the response function, we then have

$$Q_{\epsilon_1\epsilon_2\epsilon_3}^s(t_3,t_2,t_1) = -i\omega_{eg}^s(\epsilon_1 t_1 + \epsilon_3 t_3) - g_{-\epsilon_1}^s(t_1) - g_{\epsilon_2\epsilon_3}^s(t_3) - \epsilon_1\epsilon_3[g_{\epsilon_1\epsilon_2}^s(t_2) - g_{\epsilon_1\epsilon_2}^s(t_2+t_3) - g_{-\epsilon_1}^s(t_1+t_2) + g_{-\epsilon_1}^s(t_1+t_2+t_3)] \quad (8)$$

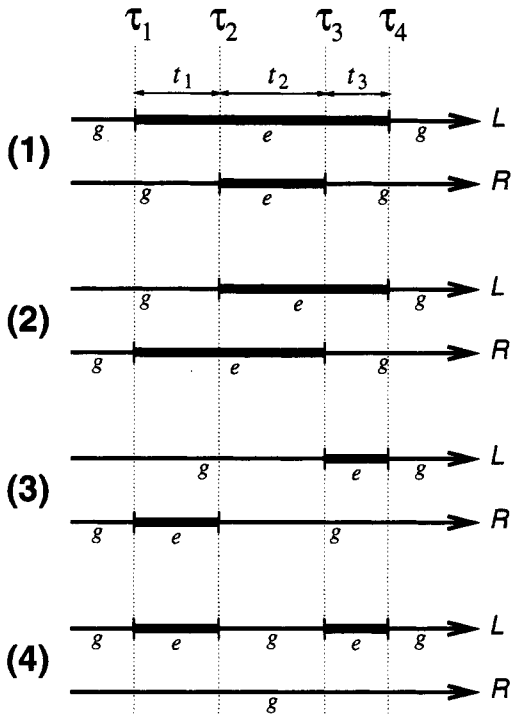

Figure 2. Double-sided Feynman diagrams in fourth order. Here, we show a coordinate representation (not phase space) of the density matrix, and, in each figure, the line with L represents a time evolutions of a ket (a left-hand side) of the density matrix, whereas the line with R represents a bra (a right-hand side) of the density matrix. The complex conjugate paths of 1–4 which can be obtained by interchanging L and R, respectively, are not shown.

TABLE I: Auxiliary Parameters ϵ_j. The System Is Initially in gg, and We Set $\epsilon_0 = -$.

Liouville space path α	ϵ_1	ϵ_2	ϵ_3
1	+ (eg)	+ (ee)	+ (eg)
2	− (ge)	+ (ee)	+ (eg)
3	− (ge)	− (gg)	+ (eg)
4	+ (eg)	− (gg)	+ (eg)

These functions are expressed by the response phase function

$$g_\pm^s(t) = \xi_s^2 \int_0^t dt' \int_0^{t'} dt'' \left[S_s(t'') \pm \frac{i\hbar}{2}\chi_s(t'')\right] \quad (9)$$

where

$$\omega_{eg}^s \equiv \omega_{eg}^0 + \lambda_s, \quad \lambda_s \equiv \frac{m_s D_s^2 \omega_s^2}{2\hbar}, \quad \xi_s = \frac{m_s D_s \omega_s^2}{\hbar} \quad (10)$$

and the antisymmetric and the symmetric position correlation functions of the ground equilibrium state for the sth mode are defined by

$$S_s(t) \equiv \frac{1}{2}\langle q_s(t)q_s + q_s q_s(t)\rangle_g = \frac{\hbar}{m_s\omega_s}\coth\left(\frac{\beta\hbar\omega_s}{2}\right)\cos(\omega_s t) \quad (11)$$

and

$$\chi_s(t) \equiv \frac{i}{\hbar}\langle q_s(t)q_s - q_s q_s(t)\rangle_g = \frac{1}{m_s\omega_s}\sin(\omega_s t) \quad (12)$$

respectively. The response function contains all the information necessary for calculating the nonlinear polarization and the optical signal.

III. Phase Space Wave Packets Determined by Using Forward Propagation

A better insight on the physical significance of the response function can be obtained by representing it as a trace over a wave

packet. The wave packet is given by the density matrix $\rho(t)$ in eq 5 expressed in the Wigner (phase space) representation. Each pathway has its own wave packet. Obviously, it carries more information than necessary for calculating the optical signal (since at the end we trace over it). Nevertheless, it reveals the underlying dynamics behind the response function and the factors affecting it. We thus recast the contribution of the α path to the response function in the form

$$R_\alpha^{(2N-1)}(t) = \int d\mathbf{p} \int d\mathbf{q}\, G_\alpha^{(2N-1)}(\mathbf{p},\mathbf{q};t) \tag{13}$$

with the corresponding wave packet

$$G_\alpha^{(2N-1)}(\mathbf{p},\mathbf{q};t) = \prod_s G_\alpha^{(2N-1)}(p_s,q_s;t) \tag{14}$$

For this model, the wave packet is a complex Gaussian function in phase space

$$G_\alpha^{(2N-1)}(p_s,q_s;\mathbf{t}) = \frac{1}{2\pi}\sqrt{\frac{1}{\langle p_s^2\rangle_g \langle q_s^2\rangle_g}} \times \exp\left[-\frac{1}{2\langle q_s^2\rangle_g}(q_s - \bar{q}_s^\alpha(\mathbf{t}))^2 - \frac{1}{2\langle p_s^2\rangle_g}(p_s - \bar{p}_s^\alpha(\mathbf{t}))^2 + Q_\alpha^s(\mathbf{t})\right] \tag{15}$$

and

$$\langle q_s^2\rangle_g = S_s(0), \qquad \langle p_s^2\rangle_g = -m_s^2 \ddot{S}_s(0) \tag{16}$$

and $\mathbf{p}$ and $\mathbf{q}$ represent a set of $\{p_s\}$ and $\{q_s\}$, respectively. Closed-form expressions for $\bar{p}_s^\alpha(t)$, $\bar{q}_s^\alpha(t)$, and $Q_\alpha^s(\mathbf{t})$ for $2N-$ l'th order are given in Appendix A. For the third-order response ($N = 2$), we have

$$\bar{q}_s^{\epsilon_1\epsilon_2\epsilon_3}(t_3,t_2,t_1) = -i\xi_s^{-1}[\epsilon_1 \dot{g}_{-\epsilon_1}^s(t_1+t_2+t_3) - \epsilon_1 \dot{g}_{\epsilon_1\epsilon_2}^s(t_2+t_3) + \epsilon_3 \dot{g}_{\epsilon_2\epsilon_3}^s(t_3)] \tag{17}$$

and

$$\bar{p}_s^{\epsilon_1\epsilon_2\epsilon_3}(t_3,t_2,t_1) = -im_s\xi_s^{-1}[\epsilon_1 \ddot{g}_{-\epsilon_1}^s(t_1+t_2+t_3) - \epsilon_1 \ddot{g}_{\epsilon_1\epsilon_2}^s(t_2+t_3) + \epsilon_3 \ddot{g}_{\epsilon_2\epsilon_3}^s(t_3)] \tag{18}$$

The functions $\bar{p}_s^\alpha(t)$ and $\bar{q}_s^\alpha(t)$ represent the contribution of the αth path to the average coordinate and momentum:

$$\bar{q}_s = \sum_\alpha q_s^\alpha \quad \text{and} \quad \bar{p}_s = \sum_\alpha \bar{p}_s^\alpha \tag{19}$$

The average coordinate and momentum are of course real, but the individual contributions $\bar{p}_s^\alpha(t)$ and $\bar{q}_s^\alpha(t)$ are complex.

IV. Phase Space Wave Packets Determined by Using Backward Propagation

So far, we have considered Liouville wave packets calculated by starting with the initial equilibrium density matrix and propagating the density matrix forward in time (from the past to the future). However, it may be possible to define wave packets corresponding to backward propagation in time. This is done as follows: We write eq 5 in the Heisenberg picture

$$P(t) = \mathrm{tr}\{V(t)\,\rho(0)\} \tag{20}$$

Calculating $V(t)$ can be carried out by starting with $V(0)$ (which is the unit operator in the nuclear space for the present model) and then propagating it in reverse order (the t_{2N-1} period is first, and the t_1 period is last). The initial state of the backward Liouville paths is a uniform distribution $G(\mathbf{p},\mathbf{q};0) = 1$. The final state, which was the initial equilibrium state in the forward case, is defined by an integration over $\mathbf{p}$ and $\mathbf{q}$ with the weight function $G_g(\mathbf{p},\mathbf{q})$, where $G_g(\mathbf{p},\mathbf{q})$ is the equilibrium state at the inverse temperature β. Denoting the backward wave packets by $D_\alpha(\mathbf{p},\mathbf{q};\mathbf{t})$, then the response function can be expressed as

$$R_\alpha^{(2N-1)}(\mathbf{t}) = \int d\mathbf{p} \int d\mathbf{q}\, D_\alpha^{(2N-1:0)}(\mathbf{p},\mathbf{q};t)\, G_g(\mathbf{p},\mathbf{q}) \tag{21}$$

where

$$D_\alpha^{(2N-1:0)}(\mathbf{p},\mathbf{q};t)\, G_g(\mathbf{p},\mathbf{q}) = \prod_s D_{\alpha s}^{(2N-1:0)}(p_s,q_s;t)\, G_g^s(p_s,q_s) \tag{22}$$

and

$$G_g^s(p_s,q_s) = \frac{1}{2\pi}\sqrt{\frac{1}{\langle p_s^2\rangle_g \langle q_s^2\rangle_g}} \times \exp\left[-\frac{1}{2\langle q_s^2\rangle_g}q_s^2 - \frac{1}{2\langle p_s^2\rangle_g}p_s^2\right] \tag{23}$$

Since the uniform initial state for $D_\alpha(\mathbf{p},\mathbf{q};\mathbf{t})$ coincides with $G_g(\mathbf{p},\mathbf{q})$ at infinite temperature, we can evaluate the backward wave packets from eq 15 by simply setting $\beta \gg \hbar\,\omega_j$ and by replacing t_{2N-1} with t_{K-J}. We thus obtain

$$D_\alpha^{(K:J)}(p_s,q_s;\mathbf{t}) = \exp[iq_s a_s^\alpha(\mathbf{t}) + ip_s b_s^\alpha(\mathbf{t}) + c_s^\alpha(\mathbf{t}) + \tilde{Q}_\alpha^s(\mathbf{t})] \tag{24}$$

The function $D^{(K:J)}(p,q;t)$ is a wave packet that starts at the interval t_K and ends at the interval t_J. In the present application, we always choose $K = 2N - 1$ and $J = 0$. The time-dependent parameters in this equation are given in Appendix B. As an example, for $K = 3$ and $J = 0$, we have

$$a_s^{\epsilon_3\epsilon_2\epsilon_1}(t_3,t_2,t_1) = \xi_s[\epsilon_3\tilde{M}_s(t_1+t_2+t_3) - \epsilon_1\tilde{M}_s(t_2+t_3) + \epsilon_1\tilde{M}_s(t_3)] \tag{25}$$

$$b_s^{\epsilon_3\epsilon_2\epsilon_1}(t_3,t_2,t_1) = \frac{\xi_s}{m_s\omega_s^2}[\epsilon_3 M_s(t_1+t_2+t_3) - \epsilon_1 M_s(t_2+t_3) + \epsilon_1 M_s(t_3)] \tag{26}$$

$$c_s^{\epsilon_3\epsilon_2\epsilon_1}(t_3,t_2,t_1) = \frac{\xi_s^2\Lambda_s}{2}[\epsilon_3\tilde{M}_s(t_1+t_2+t_3) - \epsilon_1\tilde{M}_s(t_2+t_3) + \epsilon_1\tilde{M}_s(t_3)]^2 - \frac{\xi_s^2\Lambda_s}{2\omega_s^2}[\epsilon_3 M_s(t_1+t_2+t_3) - \epsilon_1 M_s(t_2+t_3) + \epsilon_1 M_s(t_3)]^2 \tag{27}$$

and

$$\tilde{Q}_{\epsilon_3\epsilon_2\epsilon_1}^s(t_3,t_2,t_1) = -i\omega_{eg}^s(\epsilon_1 t_1 + \epsilon_3 t_3) - g_{-\epsilon_1}^s(t_1) - g_{\epsilon_2\epsilon_3}^s(t_3) - \epsilon_1\epsilon_3[g_{\epsilon_1\epsilon_2}^s(t_2) - g_{\epsilon_1\epsilon_2}^s(t_1+t_2) - g_{-\epsilon_1}^s(t_2+t_3) + g_{-\epsilon_1}^s(t_1+t_2+t_3)] \tag{28}$$

where

$$M_s(t) \equiv \frac{S_s(t)}{S_s(0)} = \cos(\omega_s t), \qquad \tilde{M}_s(t) \equiv \int_0^t M_s(t)\,dt \tag{29}$$

and $\Lambda_s = S_s(0) = \coth(\beta\hbar\omega_s/2)$.

V. Optical Signal as an Overlap of Wave Packets in Phase Space

Many optical measurements are conducted using two well-separated pulses (or groups of pulses). Examples are pump–probe, birefringence, transient grating spectroscopy, etc. In this case, the intuitive description of the process may be divided into two steps: The first pulse creates a doorway wave packet which then evolves in time. The second pulse creates another wave

packet, the window, which is related to the detection process. The signal is then given by the overlap of these two wave packets. To view the process in this intuitive manner, we need to break the description at some chosen point along the way, say t_J. We then create two wave packets: a forward wave packet which spans the time periods $t_1, t_2, ..., t_J$ and is Jth order in the field and a backward wave packet which spans the periods $t_{J+1}, t_{J+2}, ..., t_{2N-1}$ and is of order $2N-1-J$. The response function is given by these overlap of the two wave packets in phase space,

$$R^{(2N-1)}_{\epsilon_{2N-1},\epsilon_{2N-2},...,\epsilon_1}(t) = \int dp' \int dq' \, D^{(2N-1:J)}_{\epsilon_{2N-1},\epsilon_{2N-2},...,\epsilon_{J+1}}(p',q',t_{2N-1},t_{2N-2},...,t_{J+1}) \times G^{(J)}_{\epsilon_J,\epsilon_{J-1},...,\epsilon_1}(p',q';t_J,t_{J-1},...,t_1) \quad (30)$$

This decomposition, which is only possible when using the density matrix in phase space, provides a powerful starting point for developing semiclassical approximations for time-domain nuclear spectroscopies. Obviously, the former expressions are special cases of this result with the choice $J = 0$ (eq 24) or $J = 2N-1$ (eq 15).

We can break the theoretical description at will at any point (t_J) during the course of the time evolution (provided the laser fields do not overlap at that point), and rigorously recast the response function in terms of an overlap of two wave packets. Applications of this representation were made to the bond breaking in the photodissociation of ICN as measured by pump–probe spectroscopy[5] and to spectra solvated dyes.[3,12] Further applications to other techniques such as multiple ultrafast trains of pulses,[7,8] spectroscopy with phase-controlled laser,[9,13] coherent Raman, and grating spectroscopies should be most valuable.

VI. Dephasing Processes and Reduced Wave Packets

We shall now include relaxation of the optically active modes. This is commonly taken into account using the Langevin equation

$$\ddot{q}_s + \gamma_s \dot{q}_s + \omega_s^2 q_s = f_s(t) \quad (31)$$

where $f_s(t)$ is the delta correlated noise (*i.e.*, $\langle f_s(t) f_s(t')\rangle = \gamma_s \delta(t-t)/\beta$). We note, however, that quantum coherence between the bath and the vibrational system may be important at low temperatures. This effect cannot be taken into account by the classical Langevin equation, and therefore we explicitly introduce a microscopic model for a bath, which may represent optically inactive vibrational modes, phonons, solvent modes, etc. We assume that the optically active vibration is linearly coupled to an oscillator bath with the coordinates, the momentum, the mass, and the frequency of the kth bath oscillator for the sth mode and is given by x^s_k, p^s_k, m^s_k, and ω^s_k, respectively. The multimode Brownian oscillators' Hamiltonian is then expressed as

$$H_{MBO} \equiv H + \sum_s \sum_k \left[\frac{(p^s_k)^2}{2m^s_k} + \frac{m^s_k (\omega^s_k)^2}{2} \left(x^s_k - \frac{c^s_k q_s}{m^s_k (\omega^s_k)^2} \right)^2 \right] \quad (32)$$

where H is given by eq 1. Using path integral techniques, we can trace over the bath degrees of freedom and obtain a reduced description using the system q_s and p_s coordinates alone.[4] The final expression of the reduced forward wave packets is the same as eq 15. The only difference are the expressions of the correlation functions, which are now given by

$$\chi_s(t) = \frac{1}{m_s} \int_{-\infty}^{\infty} \frac{d\omega}{\pi} \frac{\omega \tilde{\gamma}_s(\omega)}{(\omega_s^2 - \omega^2)^2 + \omega^2 \tilde{\gamma}_s^2(\omega)} \sin(\omega t) \quad (33)$$

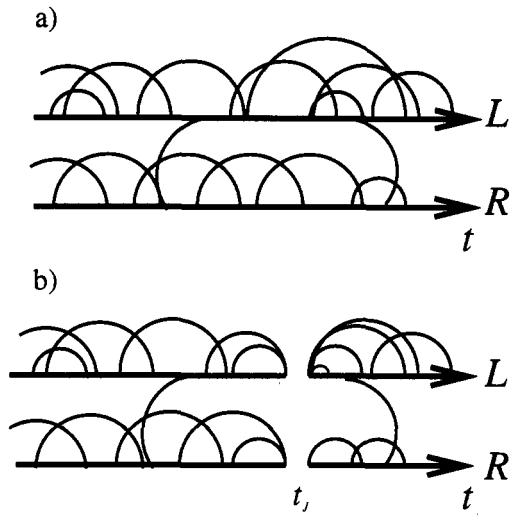

Figure 3. Schematic expression of a time evolution of the system. In each figure, the solid lines represent a time evolution of a bra and a ket of the density matrix of the nuclear system, whereas the half-circles represent phonon absorption–emission processes. The reduced wave packets, eq 15 with eqs 33 and 34, involve multiphonon emission–absorption processes as shown in Figure 3a. The factorized wave packet, eq 30 with eqs 33 and 34, however, breaks the process into two segments and neglects correlations of photon interaction processes at time t_J, as shown in Figure 3b.

and

$$S_s(t) \equiv \frac{\hbar}{m_s} \int_{-\infty}^{\infty} \frac{d\omega}{2\pi} \frac{\omega \tilde{\gamma}_s(\omega)}{(\omega_s^2 - \omega^2)^2 + \omega^2 \tilde{\gamma}_s^2(\omega)} \coth\left(\frac{\beta\hbar\omega}{2}\right) \cos(\omega t) \quad (34)$$

with

$$\tilde{\gamma}_s(\omega) \equiv \pi \sum_k \frac{(c^s_k)^2}{2m^s_k (\omega^s_k)^2} \delta(\omega - \omega^s_k) \quad (35)$$

Although the wave packet here has the same form as the previous case of the isolated system without the bath, its physical significance is profoundly different. In the present case, the wave packet provides a *reduced* description of the system where the bath degrees of the freedom have been traced over, whereas the wave packets in the previous section represent a complete description of the system. To explain the limitation of this picture, it proves convenient to write the density matrix in the coordinate representations. We define $\rho(\mathbf{q},\mathbf{q}') = \mathrm{tr}_x\{\rho(\mathbf{q},\mathbf{q}';\mathbf{x},\mathbf{x})\}$. Equations 14 and 23, etc., can be obtained by the Wigner transformation

$$G(\mathbf{p},\mathbf{q}) = \frac{1}{2\pi\hbar} \int dy \, \exp(-i\mathbf{q}y/\hbar) \, \rho(\mathbf{q}+y/2,\mathbf{q}-y/2) \quad (36)$$

The time evolution of $\rho(\mathbf{q},\mathbf{q}')$ involves multiphonon emission–absorption processes as shown in Figure 3a. In the reduced expression of the system, the phonon emitted by the bra (or ket) of the density matrix may be absorbed by ket (or bra). This is represented by the half-circle connecting the bra and the ket wave function of the system. As shown in Figure 3a, the system continuously interacts with the bath throughout the process. In eq 30, the wave packets are factorized at time $t = t_J$. Since the wave packets in the right-hand side eq 30 are in a reduced space, the process described by this factorized form neglects certain correlations between the system and bath (Figure 3b). This means that it is not generally possible to factorize the reduced wave packet. However, it may be possible to do so for some limiting cases. To find conditions for the factorization eq 30 to hold, we substituted eqs 15 and 24 into eq 30 and compared the terms in the exponent. We find that the following conditions need to be

satisfied by eq 30 to hold: (i) sufficiently high temperature of the environment, i.e., $\coth(\hbar\beta\omega_s/2) \approx 2/\hbar\beta\omega_s$, and (ii) ohmic dissipation with strong damping, $\tilde{\gamma}_s(\omega) = \gamma_s \gg \omega_s$, so that the oscillator motion is overdamped. Under these conditions, the correlation between the system and the bath is negligible and can be factorized. We may then apply the Langevin equation to describe the motion of the relaxation processes. Moreover, under these conditions the momentum may be dropped out of the description since it is always in equilibrium throughout the process. We can then replace the phase space integration $\int\int d\mathbf{p}\, d\mathbf{q}$ by a simple integration over the coordinate alone, $\int d\mathbf{q}$. This corresponds to the vibration using the Smoluchowski equation. If these conditions do not hold, we have to keep the bath degrees of freedom in our description and cannot make the factorization in the reduced space.

Acknowledgment. The supprt of the National Science Foundation and the Air Force Office of Scientific Research is gratefully acknowledged.

Appendix A: Forward Wave Packets

The Kth-order forward wave packets are given by

$$G^{(K)}_{\epsilon_1,\epsilon_2,\cdots\epsilon_K}(p_s,q_s;t) = \frac{1}{2\pi}\sqrt{\frac{1}{\langle p_s^2\rangle_g\langle q_s^2\rangle_g}}\exp\Big[-\frac{1}{2\langle q_s^2\rangle_g}\times (q_s - \bar{q}_s^{\epsilon_1,\epsilon_2,\cdots\epsilon_K}(t))^2 - \frac{1}{2\langle p_s^2\rangle_g}(p_s - \bar{p}_s^{\epsilon_1,\epsilon_2,\cdots\epsilon_K}(t))^2 + Q^s_{\epsilon_1,\epsilon_2,\cdots\epsilon_K}(t)\Big] \quad \text{(A1)}$$

where

$$\bar{q}_s^{\epsilon_1,\epsilon_2,\cdots\epsilon_K}(t) = -i\xi_s^{-1}\Big[\sum_{m=0}^{K>2m}\epsilon_{2m+1}\dot{g}^s_{\epsilon_{2m}\epsilon_{2m+1}}\Big(\sum_{l=2m+1}^{K} t_l\Big) - \sum_{m=1}^{K+1>2m}\epsilon_{2m-1}\dot{g}^s_{\epsilon_{2m}\epsilon_{2m-1}}\Big(\sum_{l=2m}^{K} t_l\Big)\Big] \quad \text{(A2)}$$

$$\bar{p}_s^{\epsilon_1,\epsilon_2,\cdots\epsilon_K}(t) = -im_s\xi_s^{-1}\Big[\sum_{m=0}^{K>2m}\epsilon_{2m+1}\ddot{g}^s_{\epsilon_{2m}\epsilon_{2m+1}}\Big(\sum_{l=2m+1}^{K} t_l\Big) - \sum_{m=1}^{K+1>2m}\epsilon_{2m-1}\ddot{g}^s_{\epsilon_{2m}\epsilon_{2m-1}}\Big(\sum_{l=2m}^{K} t_l\Big)\Big] \quad \text{(A3)}$$

$$Q^s_{\epsilon_1,\epsilon_2,\cdots\epsilon_K}(t) = -i\omega^s_{eg}\sum_{m=0}^{(K-1)/2}\epsilon_{2m+1}t_{2m+1} - \sum_{m=0}^{(K-1)/2} g^s_{\epsilon_{2m+1}\epsilon_{2m}}(t_{2j+1}) - \sum_{m=k+1}^{(K+1)/2}\sum_{k=1}^{(K-1)/2}\epsilon_{2m-1}\epsilon_{2k-1}\Big[g^s_{\epsilon_{2k}\epsilon_{2k-1}}\Big(\sum_{l=2k}^{2m-2} t_l\Big) - g^s_{\epsilon_{2k}\epsilon_{2k-1}}\Big(\sum_{l=2k}^{2m-1} t_l\Big) - g^s_{\epsilon_{2k-1}\epsilon_{2k-2}}\Big(\sum_{l=2k-1}^{2m-2} t_l\Big) + g^s_{\epsilon_{2k-1}\epsilon_{2k-2}}\Big(\sum_{l=2k-1}^{2m-1} t_l\Big)\Big] \quad \text{(A4)}$$

and

$$\langle q_s^2\rangle_g = S_s(0), \quad \langle p_s^2\rangle_g = -M^2\ddot{S}_s(0) \quad \text{(A5)}$$

Note that we set $\epsilon_0 = -$.

Appendix B: Backward Wave Packets

The Kth-order backward wave packets are given by

$$D^{(K;J)}_{\epsilon_K,\epsilon_{K-1},\cdots,\epsilon_{J+1}}(p_s,q_s;t) = \exp[iq_s a_s^{\epsilon_K,\epsilon_{K-1},\cdots,\epsilon_{J+1}}(t) + ip_s b_s^{\epsilon_K,\epsilon_{K-1},\cdots,\epsilon_{J+1}}(t) + c_s^{\epsilon_K,\epsilon_{K-1},\cdots,\epsilon_{J+1}}(t) + \tilde{Q}^s_{\epsilon_K,\epsilon_{K-1},\cdots,\epsilon_{J+1}}(t)] \quad \text{(B1)}$$

where

$$a_s^{\epsilon_K,\epsilon_{K-1},\cdots,\epsilon_{J+1}}(t) = \xi_s\Big[\sum_{m=0}^{K-J>2m}\epsilon_{K-2m}\tilde{M}_s\Big(\sum_{l=2m+1}^{K-J} t_{K+1-l}\Big) - \sum_{m=1}^{K-J-1>2m}\epsilon_{K-2m}\tilde{M}_s\Big(\sum_{l=2m}^{K-J} t_{K+1-l}\Big)\Big] \quad \text{(B2)}$$

$$b_s^{\epsilon_K,\epsilon_{K-1},\cdots,\epsilon_{J+1}}(t) = \frac{\xi_s}{m_s\omega_s^2}\Big[\sum_{m=0}^{K-J>2m}\epsilon_{K-2m}M_s\Big(\sum_{l=2m+1}^{K-J} t_{K+1-l}\Big) - \sum_{m=1}^{K-J-1>2m}\epsilon_{K-2m}M_s\Big(\sum_{l=2m}^{K-J} t_{K+1-l}\Big)\Big] \quad \text{(B3)}$$

$$c_s^{\epsilon_K,\epsilon_{K-1},\cdots,\epsilon_{J+1}}(t) = \frac{\xi_s^2\Lambda_s}{2}\Big[\sum_{m=0}^{K-J>2m}\epsilon_{K-2m}\tilde{M}_s\Big(\sum_{l=2m+1}^{K-J} t_{K+1-l}\Big) - \sum_{m=1}^{K-J-1>2m}\epsilon_{K-2m}\tilde{M}_s\Big(\sum_{l=2m}^{K-J} t_{K+1-l}\Big)\Big]^2 + \frac{\xi_s^2\Lambda_s}{2\omega_s^2}\Big[\sum_{m=0}^{K-J>2m}\epsilon_{K-2m}\times M_s\Big(\sum_{l=2m+1}^{K-J} t_{K+1-l}\Big) - \sum_{m=1}^{K-J-1>2m}\epsilon_{K-2m}M_s\Big(\sum_{l=2m}^{K-J} t_{K+1-l}\Big)\Big]^2 \quad \text{(B4)}$$

and

$$\tilde{Q}^s_{\epsilon_K,\epsilon_{K-1},\cdots,\epsilon_{J+1}}(t) = -i\omega^s_{eg}\sum_{m=0}^{(K-J-1)/2}\epsilon_{K-2m}t_{K-2m} - \sum_{m=0}^{(K-J-1)/2} g^s_{\epsilon_{K-2m}\epsilon_{K-2m-1}}(t_{K-2m}) - \sum_{m=k+1}^{(K-J-1)/2}\sum_{k=1}^{(K-J-1)/2}\epsilon_{K+2-2m}\epsilon_{K+2-2k}\times \Big[g^s_{\epsilon_{K+1-2k}\epsilon_{K-2k}}\Big(\sum_{l=2k}^{K+3-2m} t_{K+1-l}\Big) - g^s_{\epsilon_{K+1-2k}\epsilon_{K-2k}}\Big(\sum_{l=2k}^{K+2-2m} t_{K+1-l}\Big) - g^s_{\epsilon_{K-2k}\epsilon_{K-1-2k}}\Big(\sum_{l=2k-1}^{K+3-2m} t_{K+1-l}\Big) + g^s_{\epsilon_{K-2k}\epsilon_{K-1-2k}}\Big(\sum_{l=2k-1}^{K+2-2m} t_{K+1-l}\Big)\Big] \quad \text{(B5)}$$

Appendix C: Alternative Form of Response Phase Function

We first introduce

$$M_s(t) \equiv \frac{S_s(t)}{S_s(0)} \quad \text{(C1)}$$

and

$$M_s'(t) \equiv 1 - m_s\omega_s^2\int_0^t dt'\,\chi_s(t') = \int_{-\infty}^{\infty}\frac{d\omega}{\pi}\frac{\omega_s^2\tilde{\gamma}_s(\omega)}{(\omega_s^2-\omega^2)^2 + \omega^2\tilde{\gamma}_s^2(\omega)}\cos(\omega t) \quad \text{(C2)}$$

Equation 10 can be rewritten as

$$g^s_{\pm}(t) = \pm i\lambda_s[t - \int_0^t dt'\,M_s'(t')] + \Delta_s^2\int_0^t dt'\int_0^{t'} dt''\,M_s(t'') \quad \text{(C3)}$$

where we put $\Delta_s^2 = 2\lambda_s m_s\omega_s^2 S_s(0)/\hbar$.

At high temperatures ($\hbar\beta\omega_s \ll 1$), we have $\Delta_s^2 = 2\lambda_s/\beta\hbar$ and $M_s'(t) = M_s(t)$, then

$$g'^s_{\pm}(t) = \pm i\lambda_s[t - \int_0^t dt'\,M_s(t')] + \frac{2\lambda_s}{\beta\hbar}\int_0^t dt'\int_0^{t'} dt''\,M_s(t'') \quad \text{(C4)}$$

References

(1) Fano, V. *Rev. Mod. Phys.* **1957**, *29*, 74. Zwanzig, R. *Physica* **1964**, *30*, 1109.

(2) Yan, Y. J.; Mukamel, S. *J. Chem. Phys.* **1991**, *94*, 997; *Phys. Rev.* **1990**, *A41*, 6485.

(3) Mukamel, S. *Adv. Chem. Phys.* **1988**, *70*, 165. Mukamel, S. *Ann. Rev. Phys. Chem.* **1990**, *41*, 647.

(4) Tanimura, Y. and Mukamel, S. *Phys. Rev.* **1993**, *E47*, 118. Tanimura, Y. and Mukamel, S. to be published in *J. Opt. Soc. Am. B.*

(5) Yan, Y. J., Fried, L. E. and Mukamel, S. *J. Phys. Chem.* **1989**, *93*, 8149. Fried, L. E. and Mukamel, S. *J. Chem. Phys.* **1990**, *93*, 3063.

(6) Grubele, M. and Zewail, A. H. *Phys. Today* **1990**, *43*, 24.

(7) Yan, Y. X., Cheng, L. T. and Nelson, K. A. *Advances in Nonlinear Spectroscopy*; Clark, R. J. H., Hester, R. E., Eds.; Wiley: New York, 1988; p 299. Nelson, K. A. and Ippen, E. P. *Adv. Chem. Phys.* **1989**, *75*, 1. Weiner, A. M., Leaird, D. E., Wiederrecht, G. P. and Nelson, K. A. *Science* **1990**, *247*, 1317.

(8) McMorrow, D., Lotshaw, W. T., Kenney-Wallace, G. A. *IEEE J. Quantum Electron.* **1988**, *QE24*, 443. McMorrow, D. and Lotshaw, W. T. *J. Phys. Chem.* **1991**, *95*, 10395.

(9) Scherer, N. F., Ziegler, L. D. and Fleming, G. R. *J. Chem. Phys.* **1992**, *96*, 5544. Cho, M., Fleming, G. R. and Mukamel, S. *J. Chem. Phys.* **1993**, *98*, 5314. Cho, M., Du, M., Scherer, N. F., Fleming, G. R. and Mukamel, S., submitted to *J. Chem. Phys.*

(10) Lambry, J. C., Breton, J., Martin, J. L. *Nature* **1993**, 363, 320.

(11) Nibbering, E. T. J., Wiersma, D. A., Duppen, K. *Phys. Rev. Lett.* **1992**, *68*, 514.

(12) Fayer, M. D. *Annu. Rev. Phys. Chem.* **1982**, *33*, 63.

(13) Yan, Y. J., Gillian, R. E., Whitnell, R. M., Wilson, K. and Mukamel, S. *J. Chem. Phys.* **1993**, *97*, 2320.